A highly stable engineered disulfide bond in the dimer interface of *E. coli* orotate phosphoribosyl transferase

Vilius Kurauskas#, Kristoffer E. Johansson, Martin Willemoës, Jakob R. Winther†

Linderstrøm-Lang Centre for Protein Science, Department of Biology, University of Copenhagen, Ole Maaløes vej 5, DK-2200

Copenhagen N, Denmark

† Corresponding author: E-mail JRWinther@bio.ku.dk

Present address: HFD Biochemistry Laboratories, University of Wisconsin-Madison, 433 Babcock Drive, Madison, WI 53706, United States

Key words: orotate phosphoribosyltransferase, artificial disulfide bond, redox potential, thermostability;

Abbreviations: OPRT: orotate phosphoribosyl transferase; DTT_{OX}: oxidized dithiothreitol; DTT_{RED}: reduced dithiothreitol; THP: tris(hydroxymethyl)phosphine

Abstract

Structural disulfides are very rarely found in cytoplasmic proteins of mesophilic organisms. Nevertheless, disulfides can form in the cytosol if these are stabilized sufficiently by the supporting protein structure. To investigate the redox properties of structural disulfide bonds, we introduced disulfide bonds into the cytosolic enzyme from *E. coli*, orotate phosphoribosyl transferase (OPRT). Because OPRT is a homodimer the introduction of opposing cysteine residues (R44C and D92C) into separate monomers of the enzyme meant that disulfide bond formation could easily be followed by non-reducing SDS-PAGE. Redox titration experiments in DTT buffers revealed that the designed disulfide bond was exceedingly stable with a redox potential of -314 mV, close to that of dithiothreitol (DTT). This interchain disulfide bond improved global thermostability by 5.9°C relative to wild type protein and 21.4°C above its reduced form. The catalytic activity of the enzyme in either its thiol or disulfide state was not substantially affected, indicating structural integrity. Combining an inactive subunit with the asymmetric nature of disulfide bond allowed determination of rates of subunit rearrangement and disulfide formation. The R44C/D92C double mutant resulted in the formation of a symmetric homodimer with two interchain disulfides. The redox potential of this dimer variant was further decreased to -321 mV. However, the global stability of the two-disulfide dimer was not substantially increased relative to the dimer with the single disulfide bond, suggesting that the stabilizing effect was gained by preventing dimer dissociation. Finally, disulfide bond exchange is possible by thioredoxin. With a redox potential similar to that of the eukaryotic cytosol, these mutant variants may provide a new tool for cytosolic redox sensing *in vivo*, possibly targeting the thioredoxin system.

Introduction

In most living organisms the formation of structural disulfide bonds is restricted to extra-cytoplasmic compartments, e.g. periplasm, endoplasmic reticulum (ER) or intermembrane space (IMS) of mitochondria (Depuydt et al., 2011). It is generally believed that the low redox potential of the cytoplasm precludes the formation of disulfides. In general, two NADPH coupled systems are employed to ensure low cytoplasmic redox potential. The first system utilizes glutathione, where a high ratio of reduced vs. oxidized state is maintained by the enzyme glutathione reductase. Glutathione reduces disulfides to form mixed protein-glutathione disulfides, which are further resolved by glutaredoxins (Grx) (Lillig et al., 2008; Jensen et al, 2014). The cytosolic redox potential of glutathione has been measured to be around -290 mV in yeast (Ostergaard et al., 2004) and -320 mV in *Arabidopsis thaliana* (Meyer et al., 2007). In the second NADPH-dependent system, substrate disulfides are reduced by thioredoxins which in turn are reduced by thioredoxin reductase (Collet and Messens, 2010).

Multiple factors may influence the high redox potential of non-native disulfide bonds, including: 1) conformational strain induced by the formation of a non-native bond (Zhou et al., 1993), 2) low effective concentration of reacting thiol groups and 3) unfavorable electrostatic factors that affect the pK_a of the corresponding thiols. In the folded state of a protein, however, the geometry is often optimal to achieve the highest stability of structural disulfides. Thus, the effective concentration can be extremely high, and the redox potential of structural disulfides can correspondingly be very low. Although the redox potentials are known for many oxido-reductases which employ thiol-disulfide chemistry for their activity (Ortenberg and Beckwith, 2003, Fass and Thorpe, 2018), studies on the redox properties of *native structural* disulfide bonds are exceedingly scarce in scientific literature (Burton 2000, Mitchinson and Wells, 1989).

To mimic the redox properties of a structural disulfide bond, we engineered a model disulfide at the interface of a homodimeric enzyme, orotate phosphoribosyl transferase (OPRT) from *E. coli*. Since most of the naturally occurring structural disulfides are buried (Dani et al., 2003), we wanted to create a solvent exposed disulfide bond, which would be reversibly oxidized and where reduction would not significantly disrupt structure. We here describe the successful design and redox characterization of a highly stable structural disulfide whose formation is easily followed by non-reducing SDS-PAGE.

Materials and methods

Chemicals – KH_2PO_4, $MgCl_2 \cdot 6H_2O$, $FeCl_3 \cdot 6H2O$, $NaH_2PO_4 \cdot H_2O$, HCl, Na_2CO_3, $Na_2B_4O_7 \cdot 10H_2O$, ammonium persulfate and imidazole were purchased from Merck KGaA (Darmstadt, Germany). trans-4,5-Dihydroxy-1,2-dithiane (DTT_{OX}), dithiothreitol (DTT_{RED}), $(NH_4)_2SO_4$, $CaCl_2$, ampicillin sodium salt, Coomassie R250, acetic acid, 5,5'-dithiobis-(2-nitrobenzoic acid), ethylenediaminetetraacetic acid (EDTA), N-cyclohexyl-3-aminopropanesulfonic acid (CAPS), 2-(N-morpholino)ethanesulfonic acid (MES), $NiSO_4 \cdot 6H_2O$, orotic acid, 5-phospho-D-ribose 1-diphosphate pentasodium salt (PRPP), tris(hydroxymethyl)phosphine (THP), N-ethylmaleimide and sodium acetate were all products of Sigma-Aldrich GmbH (St. Louis, Missouri, USA). Isopropyl β-D-1-thiogalactopyranoside (IPTG), tris(hydroxymethyl)aminomethane (Tris), tetramethylethylenediamine, glycerol and acrylamide (30%, 37.5:1 acrylamide:bis-acrylamide) were products of AppliChem GmbH (Darmstadt, Germany). Yeast extract, agar, Pfu polymerase, molecular weight markers were purchased from Thermo Fisher Scientific (Waltham, Massachusetts, USA). Glucose was from Serva Electrophoresis GmbH (Heidelberg, Germany) and Bacto tryptone from Becton, Dickinson and Company (Franklin Lakes, New Jersey, USA). 2000 Da maleimide conjugated polyethylene glycol (mPEG-mal) was obtained from NOF Corporation (Tokyo, Japan).

Cloning, expression and purification of protein variants – mutations were introduced stepwise by the QuickChange method (Stratagene, La Jolla, California, USA) to an open reading frame of wild-type *E. coli pyrE* gene with a C-terminal His_6 tag (as described (Hansen et al., 2014). Cys-containing variants were created by replacing original codon with TGC codon for cysteine, while native Cys were replaced by GCC codons for Ala. To create an inactive enzyme variant, substitutions in the flexible loop (R99G/K100S/K103S/H105G) and in the active site D124/125N were introduced in two steps. All constructed sequences were confirmed by sequencing at Eurofins MWG Operon (Ebersberg, Germany). All the primers were designed with software provided by Stratagene and listed in the supplementary information, Table S1.

Plasmids encoding mutant OPRT variants were transformed into *E. coli* strain MRH205 (Hansen et al., 2014) which is deleted for the *pyrE* gene. Cells were grown at 37º C (after inoculation from overnight culture) in AB-LB medium (1:4 medium:flask volume) (15 mM $(NH_4)_2SO_4$, 36.5 mM Na_2HPO_4, 22 mM KH_2PO_4, 2 mM $MgCl_2$, 100 µM $CaCl_2$, 10 µM $FeCl_3$, 10% (w/v)

tryptone, NaCl, 5% (w/v) yeast extract) supplemented with 0.2% glucose and 100 µg/ml ampicillin, until OD600 of ~1 was reached. After addition of IPTG to 1 mM, cultures were grown for an additional 3.5 h at 37º C and harvested by centrifugation at 5000 g for 15 minutes. Cells were resuspended in 1/10 initial culture volume of 0.9% NaCl followed by centrifugation as above. Cell pellets were stored at -20º C. Thawed cell pellets were resuspended in 1/25 initial culture volume (20 ml) of equilibration buffer (50 mM sodium phosphate pH 8.0, 20 mM imidazole, 150 mM NaCl), sonicated on ice/water slush at 25% power for 1 minute making 2-minute breaks and repeating this 15 times using a Bandelin Electronics Sonoplus sonicator with UW 2200 ultrasonic converter and equipped with a TT 13x13 mm tip. Debris was separated by centrifugation at 12000 g for 30 minutes. Protein extract was applied to a 2 mL column of HIS-Select Nickel Affinity Gel (Sigma-Aldrich GmbH, St. Louis, Missouri, USA) equilibrated with equilibration buffer and washed with 10 mL of the same buffer. Protein was eluted with 50 mM sodium phosphate pH 8.0, 100 mM imidazole, 150 mM NaCl buffer, dialyzed twice for three hours against 50 mM Tris-HCl pH 8.0, 1 mM EDTA buffer (1:400 volume protein:buffer) at 4º C and supplemented with 50% glycerol for storage at -20º C.

Determination of disulfide redox potential – Mixtures of equal amounts of OPRT ^{C44*} and OPRT^{C92*} were equilibrated in phosphate buffer pH 7.25 with varying ratios of DTT_{RED}/DTT_{OX} (25-0.01) present in large excess over protein. The extent of disulfide bond formation in each buffer was evaluated by non-reducing SDS-PAGE as described above. The formation of a disulfide bond between the OPRT^{C44*} and OPRT^{C92*} variants were well described by a simple two-state reaction:

$$P^{-SH\ HS-}P + DTT_{OX} \rightleftarrows P^{-SS-}P + DTT_{RED} \qquad (1)$$

Where $P^{-SH\ SH-}P$ and $P^{-SS-}P$ indicates the reduced and the oxidized form of the OPRT dimer, respectively, and DTT_{OX} and DTT_{RED}, the oxidized and reduced forms of DTT, respectively. Note, that even in the reduced state OPRT is a dimer and must be treated as such in mass action equations. Thus, $K_{OX(DTT)}$ can be calculated as:

$$K_{OX(DTT)} = \frac{[P^{-SS-}P]\cdot[DTT_{RED}]}{[P^{-SH\ HS-}P]\cdot[DTT_{OX}]} \qquad (2)$$

And subsequently, standard biochemical redox potentials (E$^{o\prime}$) as determined from the Nernst equation:

$$E^{0'}_{P-SH\,HS-P} = E^{0'}_{(DTT)} - \frac{RT}{2F}\ln(K_{ox}) \quad (3)$$

Determination of disulfide bond formation kinetics – concentrated stocks of iOPRT^{C44} and OPRT^{C92}, containing 50% glycerol, were incubated with 2 mM tris(hydroxymethyl)phosphine (THP) and 2 mM reduced DTT for 30 minutes and reductants removed on a NAP5 columns (GE Healthcare, Little Chalfont, United Kingdom) equilibrated with 20 mM Tris-HCl pH 8.0, 1 mM EDTA buffer purged with argon. THP was to drive the reduction to completion. Protein concentrations were determined by absorbance at 280 nm with Nanodrop ND-1000 spectrophotometer (Thermo Fisher Scientific (Waltham, Massachusetts, USA)). To prepare a mixture for oxidizing conditions both homodimers (0.43 mg/ml of iOPRT^{C44} and 0.37 mg/ml OPRT^{C92}) were incubated with 100 µM reduced DTT (the concentration of reduced DTT was determined with Ellman's reagent, 5,5'-dithiobis-(2-nitrobenzoic acid)) in 20 mM Tris-HCl buffer pH 8.0, 1 mM EDTA for 20 minutes. Dimers were mixed and the oxidation was initiated by the addition of 10 mM oxidized DTT. Conditions for reducing conditions were prepared by incubating each homodimer separately with 2 mM of reduced DTT and 1 mM of THP for 20 minutes before mixing the homodimers together. Mixtures of both homodimers under reducing and oxidizing conditions were incubated at 30º C and aliquots were taken at different time point to measure the activity. A 15% excess of iOPRT^{C44} was used over OPRT^{C92} since the disulfide bond formation was observed not to be complete and some residual activity would remain even with prolonged incubation in oxidizing conditions.

Activity measurement was based on the decrease of orotate absorbance at 290 nm as it is converted to orotidine monophosphate by the OPRT enzyme. The assay mixture was composed of 250 µM phosphoribosyl pyrophosphate (PRPP) (concentration of active PRPP was determined by xantine phosphoribosyl phosphatase assay (Hansen et al., 2014)), 200 µM orotate and 5 mM $MgCl_2$ in 20 mM Tris-HCl pH 8.0 buffer. An aliquot of dimerization reaction mixture (under oxidizing or reducing conditions) was taken at different time points, diluted ~200 fold and 5 µl of diluted mixture was added to 145 µl of assay buffer, resulting in ~6500-fold dilution overall. Absorbance at 290 nm was measured using a Perkin-Elmer Lambda 35S (Perkin-Elmer Inc., Waltham, Massachusetts) spectrophotometer in a temperature-controlled cuvette (30º C). Initial rates were measured as decrease in absorbance over time and were obtained by linear or non-linear regression. Disulfide bond formation was assayed by quenching the samples with excess N-ethylmaleimide over DTT thiol groups and analyzing dimer monomer ratios if the samples by

non-reducing SDS-PAGE.

Oxidation by E. coli *Trx1* – Reduced iOPRT^{C44} and OPRT^{C92} were prepared by incubating concentrated protein solutions in 50% glycerol for 30 minutes with THP/DTT$_{RED}$ and desalting on a NAP5 column equilibrated with 20 mM Tris-HCl pH 8.0, 1 mM EDTA saturated with argon in argon atmosphere. 16.5 μM of each homodimer (33 μM of both homodimers) were mixed with 50 μM of *E. coli* thioredoxin 1 (Sigma-Aldrich GmbH, St. Louis, Missouri, USA), oxidized DTT or just adding Tris-HCl buffer as a control. Reaction was allowed to occur for 3 h at 30º C and aliquots were taken at different time points. Each aliquot was added to 10% trichloroacetic acid, which decreases the pH value of the solution and precipitates proteins, thus the reaction should be inhibited. Precipitated proteins were pelleted by centrifugation at 13000 g at 4º C for 1 h. Supernatant was removed, and the pellet was resuspended in 125 mM Tris-HCl, 4% SDS, 20% glycerol buffer containing bromocresol purple and 10 mM N-ethylmaleimide. 1 M Tris-HCl pH 8.0 was added to the sample until the color of bromocresol blue shifted from yellow to dark blue, indicating that the pH of the solution became optimal for N-ethylmaleimide to modify the free thiol groups. Samples were incubated for at least 15 minutes, heated to 95º C and analyzed on acrylamide gels. Band intensities of oxidized and reduced forms were quantified with ImageJ software and plotted using the R programming language.

Redox potential determination - Redox potentials were determined for iOPRT^{C44}/ OPRT^{C92}, OPRT^{C44*}/OPRT^{C92*} and OPRT$^{C44/C92*}$ disulfide bonds. The proteins were prepared for the reaction in the same way as for thioredoxin experiment, although argon atmosphere was discarded, since it was observed that 1 mM EDTA and argon purged buffers are sufficient to prevent disulfide bond oxidation by atmospheric oxygen. Furthermore, 20 mM Tris-HCl pH 8.0 buffer was substituted with 50 mM sodium phosphate, pH 7.25. A range of redox buffers was prepared, with oxidized:reduced DTT ratios (mM): 50:0.5, 25:0.5, 12.5:0.5, 5:0.5, 2.5:0.5, 1:0.5, 0.5:0.5, 0.5:1, 0.5:2.5, 0.5:5, 0.5:12.5. Each homodimer was mixed at 0.4 mg/ml with the same amount of its disulfide bond partner and 0.8 mg/ml of double mutant (OPRT$^{C44/C92*}$) and were incubated for 3 h at 30º C. Reaction was quenched the same way as for thioredoxin experiment and the samples were analyzed on acrylamide gels and quantified with ImageJ software.

Differential scanning calorimetry – Prior to determination of the thermal profiles, homodimers were reduced with THP/DTT$_{RED}$ mixture as described above and desalted. The protein concentration for differential scanning calorimetry experiments was 0.6 mg/ml (~25 μM). Full

oxidation of the disulfide bond in heterodimer mixtures (0.6 mg/ml of total protein) would require large amounts of oxidized DTT (50 mM), which might not be removed with NAP5 column and interfere with the measurements. This was indeed observed. DTT_{OX} was instead removed by micro-dialysis of a heterodimer mixture after 3 h of incubation at 30° C. About 150 μl of protein sample was subjected to 3 rounds of dialysis in 250-350-fold excess of phosphate buffer at room temperature. Full oxidation was confirmed by SDS-PAGE.

pKa determination – pKa values for $OPRT^{C44}$ and $OPRT^{C92*}$ variants were determined by analyzing their thiolate reactivities with iodoacetamide (IAM) at different pH values. 0.4 mg/ml (16.5 μM) of each variant reduced as previously. Proteins (desalted in 20 mM Tris-HCl buffer) were incubated in buffers with relatively high ionic strength to prevent electrostatic influences on thiolate reactivities and different pH values containing 1 mM of IAM for 1.5 minutes and the reaction was stopped by addition of trichloroacetic acid to 10%. Precipitated samples were incubated at 4° C for at least 15 minutes, centrifuged at 16000 g and resuspended in 125 mM Tris-HCl, 4% SDS, 20% glycerol, bromocresol purple and 2 mM mPEG-maleimide buffer. pH was increased to ~8 by addition of 1 M Tris-HCl pH 8.0 buffer and the modification of free thiol groups with mPEG was allowed to continue for 30 minutes. Following buffers containing 100 mM NaCl, 1 mM EDTA and 100 mM of buffering compound were used to make a pH scale: 5 (sodium acetate), 6 (MES), 7 (sodium phosphate), 8 (Tris-HCl), 8.5 (sodium tetraborate), 9 (sodium carbonate), 10 (CAPS), 11.3 (sodium phosphate). Samples were analyzed on 15% SDS-PAGE, two independent experiments were performed for each pH value for each of the variants. The k_{obs} values were obtained by least square regression of exponential decay of unmodified thiol and k_{S-} and pK_a values were obtained by non-linear least square approximation of the experimental data to the equation:

$$k_{obs} = \frac{k_{S^-}}{1 + 10^{pK_a - pH}} \qquad (4)$$

Results

Figure 1. OPRT with native cysteine residues shown as space filling spheres and the designed asymmetric disulfide shown as a stick model (zoomed in insert). The two subunits are shown in green and red, respectively. The active site is comprised of a binding pocket on one monomer covered by a loop (shown with arrow) on the other in a "yin-yang"-like configuration. The structure was rendered based on pdb:1ORO. The shared active site means that hetero-dimers of a wild-type subunit and a subunit lacking critical residues in both the binding pocket and the loop will be inactive.

Design of a disulfide bond – E. coli orotate phosphoribosyl transferase (OPRT) is a homodimer composed of 23.6 kDa subunits related by 2-fold symmetry. We used geometry-based algorithms (MODIP (Dani et al., 2003), Disulfide by Design (Dombkowski, 2003), BridgeD (Pellequer and Chen, 2006) on an X-ray structure of *E. coli* OPRT (PDB ID: 1ORO) (Henriksen et al., 1996) to locate putative sites for the insertion of an inter-molecular disulfide bond. All of these algorithms predicted that the cysteine substitution of opposing D92 and R44 residues would result in a left-handed disulfide bond of the most favorable geometry (Figure 1). It is important to note that in a homodimer interface the opposing residues will, in most cases, be placed at different positions in

the sequence. Small perturbations of the protein structure introduced by applying CONCOORD (de Groot et al., 1997) resulted in the C92-C44 bond still being predicted by these algorithms, indicating that the disulfide cross-link would not result in severe reduction of conformational entropy. In addition, the predicted disulfide a) interconnects helix with a coil, a feature often observed in naturally occurring disulfide bonds (De Simone et al., 2006), b) is not located in the immediate vicinity of an active site loop, the mobility of which is required for the catalytic activity of the protein, and c) is not in a region of the protein known to have any direct functional relevance (Henriksen et al., 1996).

Table 1. List of OPRTase variants with corresponding substitutions

OPRTase variant	**Characteristics**	**Substitution(s)**
$OPRT^{C44}$	Single Cys variant in active subunit	R44C
$OPRT^{C92}$	Single Cys variant in active subunit	D92C
$OPRT^{C44*}$	Single Cys variant in active subunit lacking endogeneous cysteine residues	R44C/C96A/C176A
$OPRT^{C92*}$	Single Cys variant in active subunit lacking endogeneous cysteine residues	D92C/C96A/C176A
$OPRT^{C44/C92*}$	Double Cys variant in active subunit lacking endogeneous cysteine residues	R44C/D92C/C96A/C176A
$iOPRT^{C44}$	Single Cys variant in an inactivated subunit	R44C/D124N/D125N/R99G/ K100S/K103S/H105G

To test whether we could obtain a stable disulfide bond, we generated a number of OPRT variants where residues Arg44 and Asp92 were substituted by cysteine (Table 1). Wild-type OPRT also contains two unpaired cysteine residues in each subunit (C96 and C176) which we feared might interfere. Thus, we also made R44C and D92C variants in which C96 and C176 were replaced by Ala ($OPRT^{C44*}$ and $OPRT^{C92*}$). A variant with the potential to form two inter-subunit disulfides, but lacking endogenous cysteines, was also generated ($OPRT^{C44/92*}$). Finally, a catalytically inactive C44-variant $iOPRT^{C44}$ containing mutations in both parts of the inter-subunit shared active site was also made (Table 1). Variant dimers differing in subunits by at

least one residue substitution are here referred to as *heterodimers.*

Disulfide bond formation – OPRT variants with D92C and R44C substitutions were produced as described in Materials and Methods by Ni^{2+}-affinity chromatography yielding 40-60 mg/liter of cell culture of pure hexahistidine C-terminally tagged protein for each variant in a single step (Figure S1). Incubation of equal amounts of each variant in buffers with different GSH/GSSG ratios and quenching the reaction with excess of N-ethylmaleimide resulted in a nearly complete shift of a band from ≈24 kDa (monomer) to ≈50 kDa (dimer) on non-reducing SDS-PAGE (Figure 2) indicating the formation of an intermolecular disulfide bond. Even at large molar excess of GSH the majority of the protein remained in the dimer state. Thus, it appeared that the introduced disulfide bond would be impossible to analyze with the GSH redox couple ($E^{o\prime}$ = -240 mV (Aslund et al., 1997)) as even the best commercial preparations of GSH contain a significant contamination of GSSG (Winther and Thorpe, 2014). DTT, on the other hand, has a standard biochemical redox potential ($E^{o\prime}$) of about -330 mV. Furthermore, unlike GSH, mixed disulfides with DTT are unlikely to accumulate to a significant extent (Creighton, 1986), simplifying the determination of redox potentials.

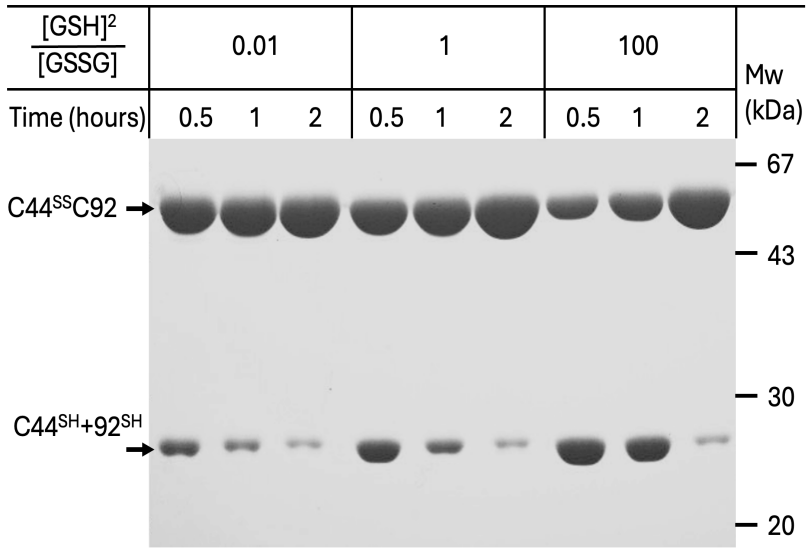

Figure 2. Formation of intermolecular disulfide bonds over time upon incubation of $OPRT^{C44}$ and $OPRT^{C92}$ with glutathione redox buffers. Disulfide bond formation is followed by non-reducing SDS-PAGE over time. Disulfide bond formation (conversion of $C44^{SH}$+$C92^{SH}$ to $C44^{SS}C92$) is relatively rapid and is almost complete even under the most reducing conditions.

Using DTT, the reversibility of the disulfide bond formation could be demonstrated, as the ratio between oxidized and reduced OPRT was only dependent only on the redox status of the buffers and independent of whether the starting point was oxidized or reduced OPRT (SI-Figure S2).

If the thiol groups were not quenched with N-ethylmaleimide prior to heating in 2% SDS sample buffer, the protein would migrate exclusively as ≈24 kDa band. This can be explained by a thiol disulfide exchange reaction with either of two Cys residues present in wild-type protein (C96 or C176), resulting in isomerization from inter- to intramolecular disulfide bond. This interpretation was indeed confirmed, because the additional introduction of C96A/C176A substitutions (to form $OPRT^{C44*}$and $OPRT^{C92*}$) resulted in migration as a dimer even when the N-ethylmaleimide was not added. Although homodimers of $OPRT^{C92}$ and $OPRT^{C44}$ were expected to be sterically unfavorable a small amount of C92-C92 and C44-C44 disulfide bonds were found if exposed to atmospheric oxygen for prolonged periods. Homodimers containing these disulfide bonds, however, exhibited different mobilities on an SDS-PAGE, and these disulfide bonds would be rapidly isomerized to more favorable C44/C92 upon the mixing of heterodimers.

Redox potential determination – Despite the abundance of attempts to introduce artificial structural disulfide bonds into proteins, redox properties of the introduced disulfides are very rarely determined. As we wished to gain more insight in the stabilities of the introduced structural disulfide bond, we next determined the redox potential of the C44-C92 disulfide couple. Thus, mixtures of equal amounts of $OPRT^{C44*}$ and $OPRT^{C92*}$ were equilibrated in phosphate buffer pH 7.25 with varying ratios of DTT_{RED}/DTT_{OX} (25-0.01) present in large excess over protein. The extent of disulfide bond formation in each buffer was evaluated by non-reducing SDS-PAGE as described above.

Non-linear least square regression to equation 2 above was used to acquire K_{OX} from experimental data. A fraction of protein migrated as a 24 kDa band even under the most oxidizing conditions, indicating that the ratio between the two cysteine variants was not perfectly balanced. This fraction was subtracted before making K_{OX} calculations. The resulting K_{OX} values for $iOPRT^{C44}$+$OPRT^{C92}$ and $OPRT^{C44*}$+$OPRT^{C92*}$, for the two variants with and without the native cysteines, respectively, were identical within the experimental error (0.286 ± 0.023 and 0.275 ± 0.025, respectively).

We also analyzed disulfide bond formation in the $OPRT^{C44/C92*}$ homodimer. As expected, this

variant exhibited the formation of a double-disulfide-bonded form, which can be seen in Figure 3B as the band with a migration rate between the reduced and single-disulfide bonded form on the gel.

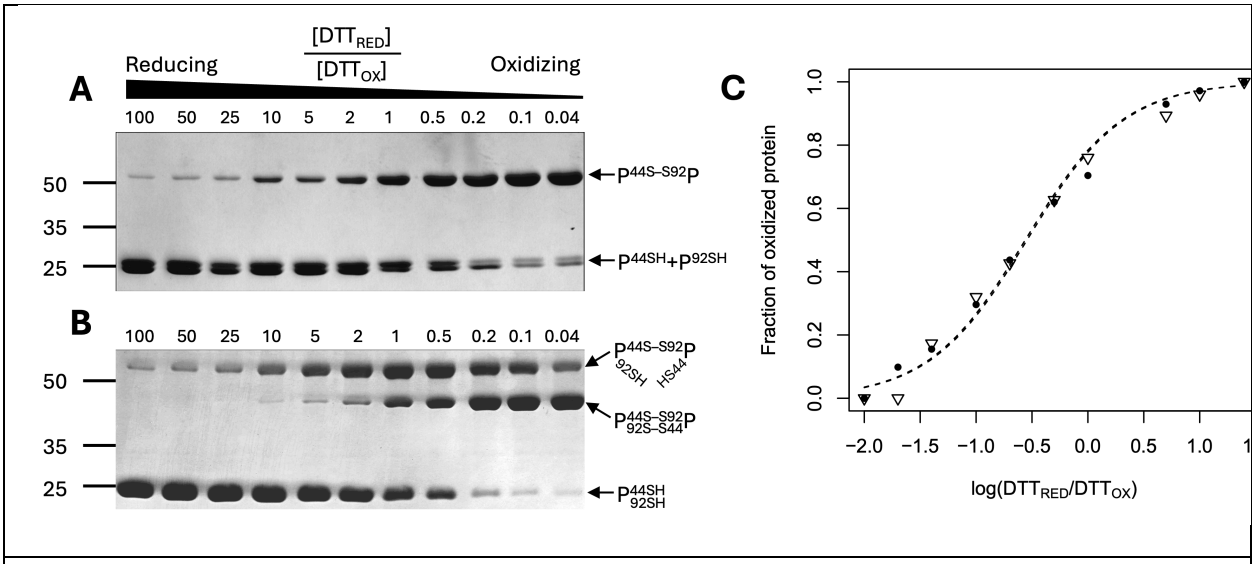

Figure 3. Redox titration of artificial disulfide bonds (**A**) Non-reducing SDS-PAGE showing $OPRT^{C92*}$+ $OPRT^{C44*}$ after exposure to varying DTT_{RED}/DTT_{OX} ratios. The disulfide-bonded heterodimer oxidized running at slightly above 50 kDa and the reduced forms at 25 kDa where the double band is likely due to the difference in charge between the two variants. (**B**) Same experiment showing $OPRT^{C44/C92*}$ after exposure to varying DTT_{RED}/DTT_{OX} ratios. From the top of the gel, the three forms represent single disulfide-bonded, double-disulfide-bonded and reduced forms, respectively. (**C**) Fraction of disulfide formation was determined from gel scans as in A for protein variants with or without the native cysteine residues ((▿) $OPRT^{C44}$+ $OPRT^{C92}$ and (●) $OPRT^{C44*}$+ $OPRT^{C92*}$, respectively). Data were fitted to a two-state redox model as described in Materials and Methods.

Adopting an E°' of -330 mV for DTT the values of E°' for disulfide bond formation are: -314 for $OPRT^{C92}$+$iOPRT^{C44}$, -313 mV for $OPRT^{C92*}$+$OPRT^{C44*}$and -329 mV for formation of the first disulfide in $OPRT^{C92*/C44*}$, respectively. It should be noted that the reactions were carried at a pH value slightly above 7 and that conditions where therefor strictly speaking not standard. However, with a pKa well above 7.5 both for DTT and the involved protein thiols (see Figure 6), K_{OX} values should not vary considerably depending on pH.

Table 2. Specific activities of the variants under different redox conditions	
Protein mixture and conditions	**Specific activity (μmol min^{-1} mg^{-1})**
OPRT^{C92}+ OPRT^{C44} (oxidized)	96
OPRT^{C92}+ OPRT^{C44} (reduced)	85
wtOPRT	89.5

Disulfide bond formation kinetics – Mixtures containing equal amounts of OPRT^{C92} and OPRT^{C44} variants under oxidizing and reducing conditions exhibited specific enzyme activities very similar to that of wild-type OPRT (Table 2), indicating the absence of gross structural perturbations, which could have been caused by the side-chain substitutions or by the formation of the disulfide bond. The activity of the reduced form of the double mutant OPRT$^{C92/C44*}$ was 7-fold lower than the wild-type enzyme, but upon oxidation of both disulfide bonds the enzyme activity was fully restored (data not shown).

To evaluate the kinetics of disulfide bond formation, an active site complementation experiment was performed similarly as done previously with OPRT from the *Salmonella typhimurium* enzyme which has 99% sequence identity to that from E. coli (Ozturk et al., 1995). The OPRT dimer contains two shared active sites, which are comprised of substrate binding site in one subunit and a covering loop from the other. Closure of the flexible loop excludes solvent water from the active site and provides K103 which is essential for catalysis (Ozturk et al., 1995). An inactive OPRT^{C44} variant (iOPRT^{C44}) was made by introducing active site substitutions in both the binding site and the flexible loop as described in Materials and Methods. Because of the yin-yang shared-active site structure of OPRT, a heterodimer between such an active-site mutant monomer and a wild-type monomer will be inactive (Ozturk et al., 1995). Thus, since only the OPRT^{C92} homodimer is active, random exchange of subunits of an active OPRT^{C92} dimer and iOPRT^{C44} variant would result in a time-dependent decrease of activity, reaching 50% of initial activity when the two different modified subunits are randomly mixed in the absence of disulfide bond formation. However, on shift to oxidizing conditions, the activity should over time approach zero, since the conversion to heterodimer would be driven by disulfide bond formation.

This is indeed observed (Figure 4A). In the experiment shown in Figure 4A a 15% excess of the iOPRT^{C44} (inactive) over OPRT^{C92} (active) was used to compensate for incomplete disulfide bond formation under the experimental conditions applied (Figure 4B) and relatively high residual activity was seen even after prolonged incubation of heterodimer under oxidizing conditions.

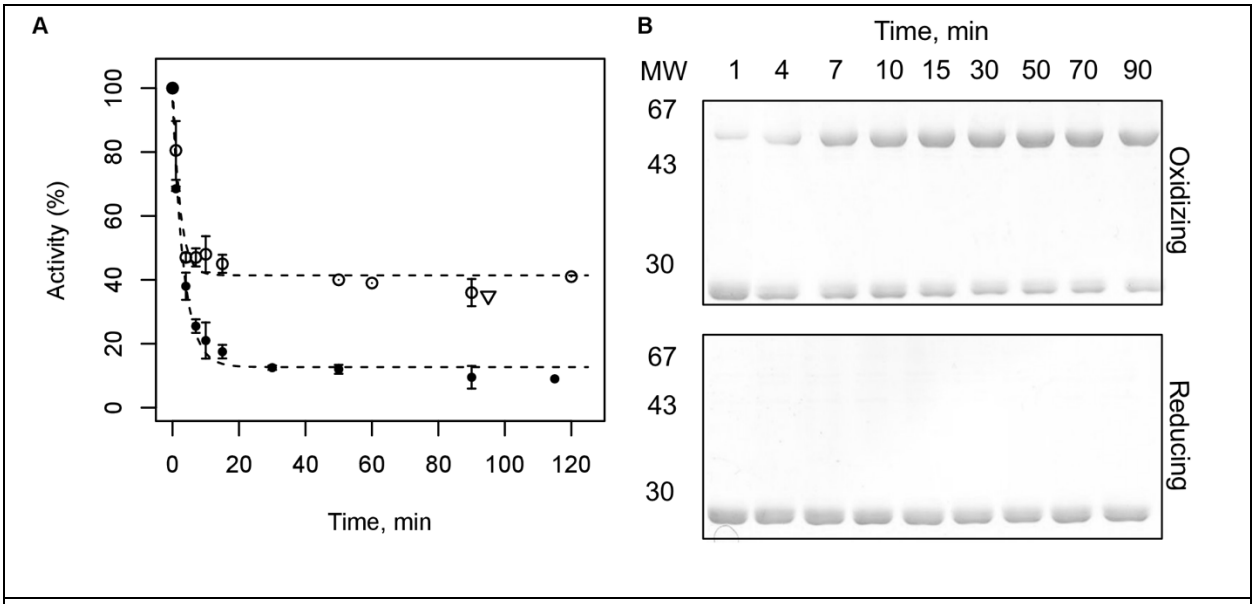

Figure 4. Kinetics of disulfide bond formation analyzed by negative active-site complementation. (A) At the start of the reaction the OPRT^{C92} homo-dimer represents 100% activity. Negative active site complementation of iOPRT^{C44} and OPRT^{C92} under reducing (○) and oxidizing (●) conditions reduces activity to half by random association active and inactive species due to formation of an oxidized heterodimer. The activity of this oxidized heterodimer is restored after 10-minute reduction with THP (▽). Dotted lines indicate single exponential fit and error bars indicate one standard deviation. (B) Non-reducing SDS-PAGE as in figure 1. The formation of disulfide bonds in the OPRT^{C92} and iOPRT^{C44} heterodimer is followed over time under oxidizing and reducing conditions. A small fraction of homodimer after 90 min is attributed to slight deviation from equimolar amounts of the two variants.

The rate-limiting step for the exchange of monomers in a dimer could, in principle, be dictated by either dissociation or association rates of the subunits. Ozturk et al. have shown that indeed the dissociation is limiting the exchange rate for OPRT monomers (Ozturk et al., 1995). Hence, if the disulfide bond formation is slower than the rate of dissociation, the rate of activity decay should be considerably different between oxidizing and reducing conditions since complete formation of the heterodimer is driven by disulfide bond formation. To compare rates, the

activity decay is modeled as a first order reaction (Figure 4A, dashed lines), rate constants describing the decrease of activity of reduced and oxidized mixtures are not significantly different, being 0.45±0.21 min^{-1} for reduced disulfide and 0.3±0.085 min^{-1} for oxidized. Therefore, the rate of disulfide bond formation must be limited by dimer dissociation. These rate constants of disulfide bond formation are in good agreement with the ones calculated from the disulfide bond formation observed on acrylamide gels (0.22±0.09 min^{-1}) (Figure 4B).

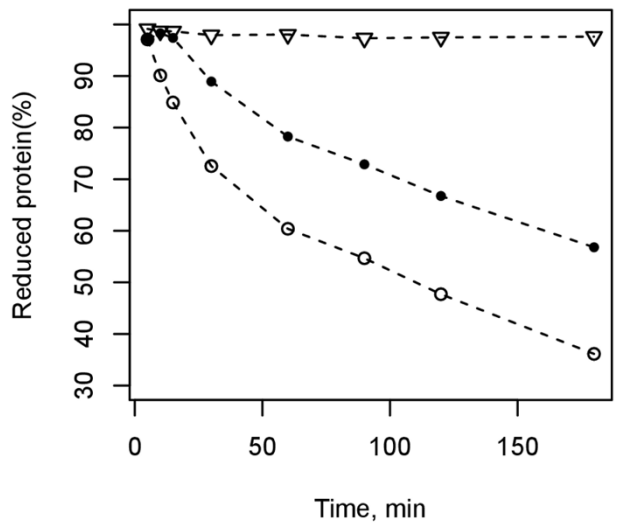

Figure 5. Kinetics of oxidation of $OPRT^{C92*}$ and $OPRTC^{44*}$ with thioredoxin. A 1:1 mixture of 16.5 μM of $OPRT^{C92*}$ and $OPRT^{C44*}$ was mixed with 50 μM of DTT_{OX} (●) or 50 μM *E. coli* thioredoxin 1 (○), respectively. A control experiment without addition of oxidant is also shown (▽).

Oxidation by thioredoxin – The observation that redox potential for the C44/C92 disulfide was very low prompted us to test if the *E. coli* thioredoxin, *Trx1,* could oxidize this disulfide bond. Even though *Trx1* has one of the lowest redox potentials (-290 mV) determined for any CXXC active site redox catalysts (El Hajjaji et al., 2009), the oxidation of the artificial OPRT disulfide bond should still be thermodynamically favorable. To test this, 3-fold excess of oxidized thioredoxin was mixed with reduced $iOPRT^{C44}/OPRT^{C92}$ heterodimer under oxygen-free conditions at pH 8.0 and oxidation of the disulfide bond was followed over time by quenching with N-ethylmaleimide followed by non-reducing SDS-PAGE. DTT_{OX} was used as a low-molecular weight oxidant control. While no significant oxidation occurred in the absence of oxidized thioredoxin and DTT_{OX}, addition of either of the components resulted in the oxidation

to form a disulfide bond (Figure 5). No mixed disulfides were observed between OPRT monomers and Trx (Figure S3) showing, not surprisingly, that the half-life of this intermediate is short. In spite of possible steric hindrance, the rate of disulfide bond formation was significantly faster in Trx-containing mixture compared to DTT_{OX} mixture at identical concentrations of the oxidant. This demonstrates that oxidation of the disulfide bond is indeed catalyzed by Trx, albeit not at high rate.

pKa determination – In the $OPRT^{C44}$ homodimer C44 is located at the N-terminal end of an α-helix, therefore the thiolate should be stabilized by a positive dipole of the helix but is, on the other hand, proximal to D92 on the opposing monomer. Inversely, C92 resides near a positively charged arginine on the opposing monomer.

The pKa values of the thiol groups of $OPRT^{C44*}$ and $OPRT^{C92*}$ variants, iodoacetamide was used as a thiol modifying agent essentially as described previously (Iversen et al, 2010). In this assay, the reactivity of iodoacetic acid is dependent on the protonation state of thiolate and the pK_a can thus be determined from the reaction rates at different pH values. The degree of iodoacetamide modification is determined by subsequent labeling with mPEG-maleimide, which increases the molecular weight of the unreacted protein by 2 kDa. The extent of modification can thus be visualized by analyzing samples by SDS-PAGE. While the thiol group of $OPRT^{C44*}$ was fully modified with mPEG-maleimide (Figure S4), only ~50% mPEG-maleimide modification was seen for the $OPRT^{C92*}$ thiol even at low pH. Here it should be essentially nonreactive towards iodoacetamide and thus undergo full mPEG modification. Although we cannot explain this loss of reactivity, it can be reasoned that the same amount of the thiol was not participating in the reaction in all of the samples. Hence, the fraction of unreacted protein was subtracted, and the extent of modification was normalized.

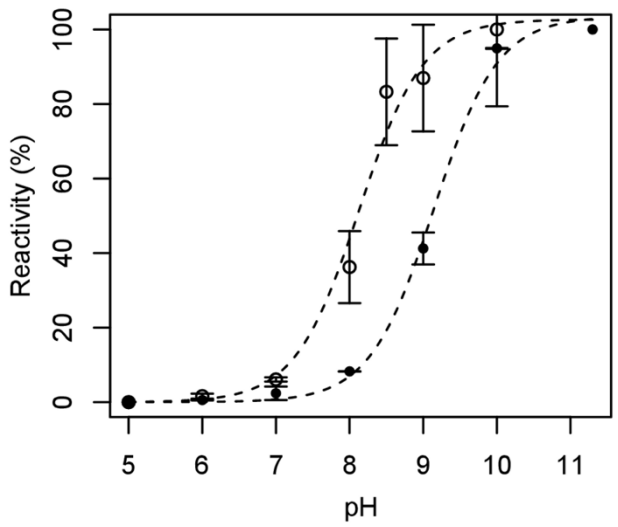

Figure 6. Determination of thiol pKa values for the two cysteines introduced. The pH dependence of the relative reaction rates of (○) - OPRT^{C92*} and (●) - OPRT^{C44*} thiols is shown. Dashed lines indicate the non-linear least squares estimation as described in the text and show a pKa of 8.1 for Cys92 and 9.1 for Cys44. Error bars indicate one standard deviation.

The pK_a values obtained for C44 and C92 thiols were in good agreement with initial predictions, being 9.14±0.05 and 8.12±0.1 respectively (Figure 6). Maximal reaction rates, k_{S^-} values, on the other hand, were essentially the same, being 1.5 $M^{-1}min^{-1}$ for both thiols.

Determination of global thermostability – The influence of disulfide bond on the stability of proteins was analyzed with differential scanning calorimetry (Figure 7; Table 3). One peak was observed for all the protein variants in a range of 30 to 90º C (Figure 7), followed by a very intense heat emission which is indicative of protein aggregation. Twofold reduction or increase in protein concentration did not affect the position of the peak, suggesting the dimer-monomer equilibrium is not part of the unfolding pathway but more likely that dissociation and unfolding are concerted reactions.

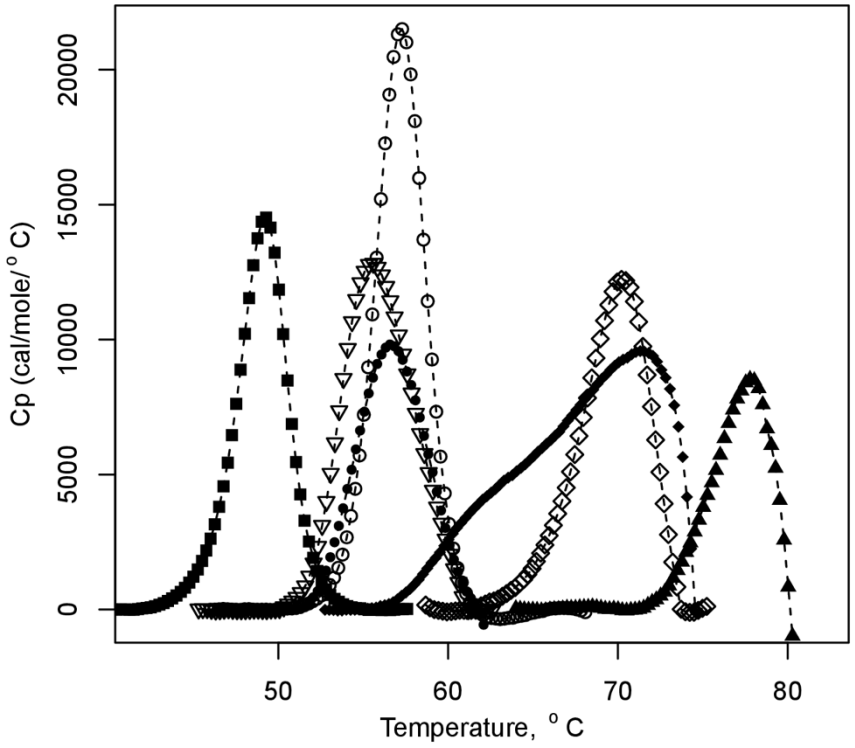

Figure 7. Thermal unfolding profiles of protein variants, iOPRT^{C44} (■), OPRT^{C44*} (▿), OPRR^{C92} (○), OPRT^{C92*} (●), wtOPRT (♦), OPRT^{C92*} + OPRT^{C44*} (oxidized, (◊)) and OPRT$^{C44/C92*}$ (oxidized, (▲)). It can be seen, that oxidized OPRT forms are at least as stable as wild-type protein, however, reduced forms have decreased stability relative to wild-type.

The heat denaturation of all of the variants, including wtOPRT, was irreversible, allowing to obtain only T_m of denaturation. The wtOPRT melting profile displayed a shoulder (Figure 7), which could indicate dimer dissociation prior to unfolding. A mixture of OPRT^{C92} and OPRT^{C44} variants under reducing conditions displayed almost identical unfolding profiles as corresponding variants analyzed individually, thus only the stabilities of homodimers are presented in Figure 7. Notably, all the cysteine variants were less stable than the wild type-protein in the absence of a disulfide bond, but the thermal stability was restored to wtOPRT level, or above, upon formation of the disulfide bond. Interestingly, OPRT$^{C92/C44*}$ with both disulfide bonds oxidized did not increase the stability substantially compared to oxidized OPRT^{C92*}+OPRT^{C44*} having only a single disulfide. On the other hand, OPRT$^{C92/C44*}$ was stabilized to the largest extent (26.4 ºC) when compared to its reduced form.

Table 3. T_m values obtained from differential scanning calorimetry	
Variant	**T_m ºC**
$OPRT^{C92}$	57.1
$OPRT^{C92}$ + $iOPRT^{C44}$ (oxidized)	69.9
$OPRT^{C92*}$	56.7
$OPRT^{C44*}$	55.1
$OPRT^{C92*}$ + $OPRT^{C44*}$ (oxidized)	77.4
$OPRT^{C44/C92*}$ (reduced)	52.2
$OPRT^{C44/C92*}$ (oxidized)	78.6
wtOPRT	71.5

Discussion

We have successfully designed a very stable disulfide bond. The designed disulfide bond is expected to have dihedral angle values (X^1: -64°/-70°, X^2: 141°/-56.5°, X^{SS}: -74°), which are well populated among naturally occurring structural disulfides (Dani et al., 2003; Petersen et al., 1999). Its conformation is predicted to have low dihedral strain energy (Marques et al., 2010), which was observed experimentally by relatively low redox potential close to that of DTT. Although it is an intermolecular cross-link in a strict sense, a strong protein dimerization, as seen for OPRT, increases the effective concentration of reacting thiols by positioning them in a close spatial proximity. As a result, low redox potential observed for the disulfide bond is more akin to intra-chain disulfides. It was observed that the disulfide bond isomerizes from intermolecular to intramolecular when the protein is heated in the presence of SDS. This behavior is expected, since the disruption of dimer interface highly reduces the probability of encounter between C92 and C44 thiol groups, largely diminishing the rate of the formation for of this particular disulfide bond, while disrupted structure and increased protein backbone mobility makes it more likely that native C96 and/or C176 thiols attack the disulfide bond.

As indicated by differential scanning calorimetry, the disulfide bond stabilized the $OPRT^{C44*}$-$OPRT^{C92*}$ dimer relative to the wild-type protein by approximately 6° C. However, geometry-based algorithms did not predict a large destabilization of the reduced form. Taking a thermodynamic cycle into consideration (Kim and Lin, 1989), the stability of the disulfide bond will be increased by decreasing the ΔΔG for unfolding of the reduced form of the Cys-containing species, as long as the native reduced state is more stable than the unfolded state. Therefore, it seems likely that geometry-based algorithms optimizing the oxidized state of the disulfide bond, but disregarding stabilities of half-cystines, are likely to improve the stability of disulfide bonds themselves, but not the proteins into which they are introduced. The program for disulfide bond prediction, BridgeD (Pellequer and Chen, 2006), attempts to evaluate the destabilizing effect of substitutions. Nevertheless, the contribution of exposed salt bridges (as the putative one between R44 and D92) to the stabilization of proteins is controversial (Dong and Zhou, 2002) and the program BridgeD highly overestimated the free energy cost of C44/C92 substitutions, giving a disulfide bond relatively low ranking.

Substitutions had a profound influence on the stability of the reduced protein, destabilizing mutant variants by ~16º C for one introduced substitution and ~20º C when both substitutions are introduced. A steric "clash", as it is often proposed to explain destabilizing effect of unsuccessfully introduced disulfide bonds (Mitchinson and Wells, 1989), would be unlikely, since a cysteine residue has only slightly bigger volume ($V_r \approx 103$ Å^3) than Asp ($V_r \approx 91$Å^3) and is much smaller than Arg ($V_r \approx 150$ Å^3) (Creighton, 1994). Therefore, disruption of a salt bridge between Arg-Asp residues seems to be a more likely explanation for the reduced stability of the reduced form. These results demonstrate the potential complications associated with the introduction of disulfide bonds in proteins with the purpose of enhancing stability.

The intrinsic reactivities of C44 and C92 towards IAM were very similar (k_{obs} values 1.5 s^{-1}), indicating, that the residues should be equally surface accessible. Lowered pK_a value for C92 (8.12 compared to ~9 for cysteines in peptides) could be explained by its proximity to the positively charged Arg residue in the homodimer of $OPRT^{C92*}$. The pK_a value of C44 is expected, since the N-terminus of a dipole of an α-helix could compensate for the destabilizing effect by the negatively charged D92 (Wada, 1976).

The surface accessibility of our engineered disulfide bond contrasts to naturally occurring disulfides, which are generally buried (Dani et al., 2003). The latter property hampers analysis of

redox potential, and explains why most, if not all, well characterized disulfide bonds are from designs. Thus, the engineered C60-C173 disulfide of human carbonic anhydrase II has a redox potential of -337 mV (calculated from K_{ox} with DTT), although the oxidized protein is less stable than wild-type (Burton et al., 2000). Mitchinson and Wells introduced a series of disulfide bonds to subtilisin BPN', several of which were extremely stable (Mitchinson and Wells, 1989).

To the best of our knowledge, the redox potential of $OPRT^{C44/C92*}$ is the lowest determined for a designed *intermolecular* disulfide bond. The fact that it is intermolecular makes it an attractive tool for determination of intracellular redox status as the level of disulfide bond formation can readily be determined from immunoblots of non-reducing SDS-PAGE. An intramolecular disulfide bond engineered into Yellow Fluorescent Protein (rxYFP) had a redox potential of -265 mV as determined by equilibration with glutathione and was present in the cytoplasm of eukaryotes at 10-15% (Ostergaard et al., 2001; Ostergaard et al. 2004). The roGFP1 and 2 sensors have redox potentials of -288 and -272 mV respectively (Hanson et al., 2004). The fact that these redox probes are all to some extent oxidized in the cytosol of eukaryotic cells suggest that $OPRT^{C44/C92*}$ likely to be even more so provided it was at equilibrium with the glutathione. However, while GFP based probes are not substrates for thioredoxin, $OPRT^{C44/C92*}$ is. It will be interesting to determine the redox state of this probe in living cells, to reveal whether the kinetic link to the thioredoxin pathway will display a different redox potential than that previously uncovered by rxYFP and roGFP's.

References

Aslund F, Berndt KD, Holmgren A (1997), Redox potentials of glutaredoxins and other thiol-disulfide oxidoreductases of the thioredoxin superfamily determined by direct protein-protein redox equilibria, J Biol Chem; 272(49):30780-6

Beeby M, O'Connor BD, Ryttersgaard C, Boutz DR, Perry LJ, Yeates TO (2005), The genomics of disulfide bonding and protein stabilization in thermophiles, PLoS Biol;3(9):e309

Burton RE, Hunt JA, Fierke CA, Oas TG (2000), Novel disulfide engineering in human carbonic anhydrase II using the PAIRWISE side-chain geometry database, Protein Sci;9(4):776-

Collet JF, Messens J (2010), Structure, function, and mechanism of thioredoxin proteins, Antioxid Redox Signal. 2010 Oct;13(8):1205-16

Creighton TE (1993). Proteins: structures and molecular properties. W.H. Freeman and Company, New York.

Creighton TE (1986), Disulfide bonds as probes of protein folding pathways, Methods Enzymol;131:83-106

Dabir DV, Leverich EP, Kim SK, Tsai FD, Hirasawa M, Knaff DB, Koehler CM (2007), A role for cytochrome c and cytochrome c peroxidase in electron shuttling from Erv1, EMBO J. 2007 Nov 28;26(23):4801-11

Dani VS, Ramakrishnan C, Varadarajan R (2003), MODIP revisited: re-evaluation and refinement of an automated procedure for modeling of disulfide bonds in proteins, Protein Eng;16(3):187-93

de Groot BL, van Aalten DM, Scheek RM, Amadei A, Vriend G, Berendsen HJ (1997), Prediction of protein conformational freedom from distance constraints, Proteins;29(2):240-51

De Simone A, Berisio R, Zagari A, Vitagliano L (2006), Limited tendency of alpha-helical residues to form disulfide bridges: a structural explanation, J Pept Sci. 2006 Dec;12(12):740-7

Depuydt M, Messens J, Collet JF (2011), How proteins form disulfide bonds, Antioxid Redox Signal. 2011 Jul 1;15(1):49-66

Dombkowski AA (2003), Disulfide by Design: a computational method for the rational design

of disulfide bonds in proteins, Bioinformatics;19(14):1852-3

Dong F and Zhou HX (2002), Electrostatic contributions to T4 lysozyme stability: solvent-exposed charges versus semi-buried salt bridges, Biophys J., 83(3): 1341-7

Fass D, Thorpe C (2018), Chemistry and enzymology of disulfide cross-linking in proteins. Chemical reviews., 118(3):1169-98

El Hajjaji H, Dumoulin M, Matagne A, Colau D, Roos G, Messens J, Collet JF (2009), The zinc center influences the redox and thermodynamic properties of Escherichia coli thioredoxin 2. Journal of molecular biology, 386(1):60-71.

Hansen, MR, Barr, EW, Jensen, KF, Willemoës, M, Grubmeyer, C, & Winther, JR (2014). Catalytic site interactions in yeast OMP synthase. Arch. Biochem. Biophys.;542, 28-38.

Hanson, GT, Aggeler, R, Oglesbee, D, Cannon, M, Capaldi, RA, Tsien, RY, & Remington, SJ (2004). Investigating mitochondrial redox potential with redox-sensitive green fluorescent protein indicators. *J Biol Chem*, *279*(13), 13044-13053.

Henriksen A, Aghajari N, Jensen KF, Gajhede M (1996), A flexible loop at the dimer interface is a part of the active site of the adjacent monomer of Escherichia coli orotate phosphoribosyltransferase, Biochemistry;35(12):3803-9

Iversen, R, Andersen, PA, Jensen, KS, Winther, JR, Sigurskjold, BW (2010). Thiol− disulfide exchange between glutaredoxin and glutathione. Biochemistry; 49(4): 810-820.

Jensen KS, Hansen RE, Winther JR (2009), Kinetic and thermodynamic aspects of cellular thiol-disulfide redox regulation, Antioxid Redox Signal;11(5):1047-58

Jensen KS, Pedersen JT, Winther JR, Teilum K (2014). The pKa value and accessibility of cysteine residues are key determinants for protein substrate discrimination by glutaredoxin. Biochemistry; 53(15):2533-40.

Lillig CH, Berndt C, Holmgren A (2008), Glutaredoxin systems, Biochim Biophys Acta;1780(11):1304-17

Lin TY, Kim PS (1989), Urea dependence of thiol-disulfide equilibria in thioredoxin: confirmation of the linkage relationship and a sensitive assay for structure. Biochemistry; 28(12):5282-7.

Marques JR, da Fonseca RR, Drury B, Melo A (2010), Conformational characterization of disulfide bonds: a tool for protein classification, J Theor Biol;267(3):388-95

Meyer AJ, Brach T, Marty L, Kreye S, Rouhier N, Jacquot JP, Hell R (2007), Redox-sensitive GFP in Arabidopsis thaliana is a quantitative biosensor for the redox potential of the cellular glutathione redox buffer, Plant J;52(5):973-86

Mitchinson C, Wells JA (1989), Protein engineering of disulfide bonds in subtilisin BPN', Biochemistry;28(11):4807-15

Ortenberg R, Beckwith J (2003), Functions of thiol-disulfide oxidoreductases in *E. coli*: redox myths, realities, and practicalities, Antioxid Redox Signal;5(4):403-11

Ostergaard H, Henriksen A, Hansen FG, Winther JR (2001), Shedding light on disulfide bond formation: engineering a redox switch in green fluorescent protein, EMBO J;20(21):5853-62

Ostergaard H, Tachibana C, Winther JR (2004), Monitoring disulfide bond formation in the eukaryotic cytosol, J Cell Biol.;166(3):337-45

Ozturk DH, Dorfman RH, Scapin G, Sacchettini JC, Grubmeyer C (1995), Structure and function of Salmonella typhimurium orotate phosphoribosyltransferase: protein complementation reveals shared active sites, Biochemistry; 34:10764-70

Pellequer JL, Chen SW (2006), Multi-template approach to modeling engineered disulfide bonds, Proteins. 2006 Oct 1;65(1):192-202

Petersen MT, Jonson PH, Petersen SB (1999), Amino acid neighbours and detailed conformational analysis of cysteines in proteins, Protein Eng. 1999 Jul;12(7):535-48

Wada A (1976), The alpha-helix as an electric macro-dipole. Advances in biophysics; 1:1-63.

Winther, JR, & Thorpe, C (2014), Quantification of thiols and disulfides. Biochim Biophys Acta (BBA)-Gen Subj;1840(2):838-846.

Zhou NE, Kay CM, Hodges RS (1993), Disulfide bond contribution to protein stability: positional effects of substitution in the hydrophobic core of the two-stranded alpha-helical coiled-coil, Biochemistry;32(12):3178-87